REPORTS

OPTICS

Microresonator soliton dual-comb spectroscopy

Myoung-Gyun Suh,* Qi-Fan Yang,* Ki Youl Yang, Xu Yi, Kerry J. Vahala†

Measurement of optical and vibrational spectra with high resolution provides a way to identify chemical species in cluttered environments and is of general importance in many fields. Dual-comb spectroscopy has emerged as a powerful approach for acquiring nearly instantaneous Raman and optical spectra with unprecedented resolution. Spectra are generated directly in the electrical domain, without the need for bulky mechanical spectrometers. We demonstrate a miniature soliton-based dual-comb system that can potentially transfer the approach to a chip platform. These devices achieve high-coherence pulsed mode locking. They also feature broad, reproducible spectral envelopes, an essential feature for dual-comb spectroscopy. Our work shows the potential for integrated spectroscopy with high signal-to-noise ratios and fast acquisition rates.

Since their demonstration in the late 1990s (*1*–*3*), optical frequency combs have revolutionized precision measurements of time and frequency and have enabled new technologies such as optical clocks (*3*). One remarkable method they make possible is dual-comb spectroscopy, which leverages the coherence properties of combs for rapid broadband spectral analysis with high accuracy (*4*–*10*). Frequency comb systems exist across a broad spectral range spanning ultraviolet to infrared, making this method well suited for measurement of diverse molecular species (*10*).

In parallel with advancements in frequency comb applications, the past decade has witnessed the appearance of miniature optical frequency combs or microcombs (*11*, *12*). These microcombs have been demonstrated using several dielectric materials across a range of emission bands (*11*, *13*–*17*). Under continuous-wave laser pumping, the combs are initiated by way of parametric oscillation (*18*, *19*) and are broadened by cascaded four-wave mixing (*11*, *12*) to spectral widths that can encompass an octave of spectrum (*15*). Four-wave mixing in the ultrafast intraband gain medium of quantum cascade lasers has also been shown to create frequency modulation (FM) combs (*20*). These FM systems have been applied to demonstrate dual-comb spectroscopy in the mid-infrared (*21*). Also, heterodyne of two conventional microcombs in the mid-infrared has been demonstrated, a key step toward dual-comb spectroscopy (*22*).

A major advancement in microcombs has been the realization of soliton mode locking (*23*–*27*). Soliton microcombs feature dissipative Kerr solitons that leverage the Kerr nonlinearity to both compensate dispersion and overcome cavity loss by way of parametric gain (*23*). Unlike earlier microcombs, this new device provides phase-locked femtosecond pulses with well-defined, repeatable spectral envelopes, which is important for dual-comb spectroscopy. The pulse repetition rate of the device is detectable, and it has excellent phase noise characteristics (*24*). In this work, we demonstrate dual-comb spectroscopy using this new platform. The dual-comb source spans >30 nm and the interferogram spectra feature high signal-to-noise ratios (SNRs). Also, precise microfabrication control enables close matching of the repetition rates so that >4 THz of optical bandwidth is measured within 500 MHz of electrical bandwidth.

A schematic view of the dual-comb experimental setup (Fig. 1) shows two soliton trains having different repetition rates ($\Delta f_r = f_{r1} - f_{r2}$) generated from distinct microresonators and then combined using a directional coupler. One of the combined streams is coupled through a gas cell of molecules (test sample in the figure) whose absorption spectrum is to be measured. The other combined stream provides a reference. The slight difference in repetition rates of the soliton streams creates a periodically time-varying interferogram in the detected current with a period $1/\Delta f_r$. Fourier transform of this time-varying signal reveals the interfering soliton comb spectra, now shifted to radio-frequency rates. The signal spectrum containing the molecular absorption information is then normalized using the reference spectrum to reveal the spectral absorption of the gas cell. [See (*28*) for details of the experimental setup, methods, and equipment.]

Solitons are generated and stabilized in two microresonators by means of the active-capture/locking technique (fig. S1) (*24*, *28*). The locking makes it possible for the two combs to remain stable indefinitely. Typical soliton optical spectra (Fig. 2, A and B) feature the characteristic sech^2 envelope, observed in this case over a 60-nm wavelength span. The detected electrical spectrum for each soliton source was measured using a spectrum analyzer with a bandwidth of 26 GHz (Fig. 2, C and D). The narrow spectral lines (resolution bandwidth of 500 Hz) have SNRs greater than 75 dB, which shows that the corresponding repetition rates are extremely stable. The high-Q resonators used in this work are silica whispering-gallery devices fabricated on a silicon wafer by a combination of lithography and wet/dry etching (*29*). The unloaded quality factor of the microresonators is approximately 300 million, and the solitons have repetition rates of approximately 22 GHz that were determined primarily by the diameter of the devices (3 mm).

The optical outputs from the stabilized soliton sources are combined and coupled into two paths (Fig. 1 and fig. S1). One path contains a $H^{13}CN$ gas cell (*28*), which functions as the test sample in the

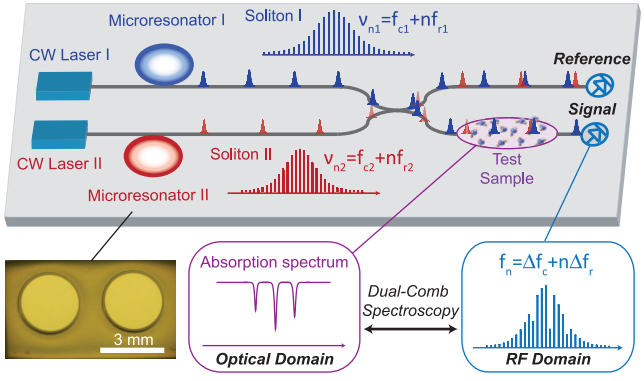

Fig. 1. Microresonator-based dual-comb spectroscopy. Two soliton pulse trains with slightly different repetition rates are generated by continuous-wave (CW) laser pumping of two microresonators. The pulse trains are combined in a fiber bidirectional coupler to produce a signal output path that passes through a test sample as well as a reference output path. The output of each path is detected (on Reference and Signal photo detectors) to generate an electrical interferogram of the two soliton pulse trains. The interferogram is Fourier-transformed to produce comb-like radio-frequency (RF) electrical spectra having spectral lines spaced by the repetition rate difference of the soliton pulse trains. The absorption features of the test sample can be extracted from this spectrum by normalizing the signal spectrum by the reference spectrum. Also shown are two silica disk resonators. The disks have a diameter of 3 mm and are fabricated on a silicon chip. The *n*th optical comb frequency (ν_{n1} and ν_{n2}) for each soliton pulse train is given in terms of the respective repetition rate (f_{r1} and f_{r2}) plus an offset frequency (f_{c1} and f_{c2}). In the RF domain spectrum, the *n*th line occurs at a multiple of the difference in the repetition rates ($\Delta f_r = f_{r2} - f_{r1}$) plus an offset frequency ($\Delta f_c = f_{c2} - f_{c1}$).

T. J. Watson Laboratory of Applied Physics, California Institute of Technology, Pasadena, CA 91125, USA.
*These authors contributed equally to this work.
†Corresponding author. E-mail: vahala@caltech.edu

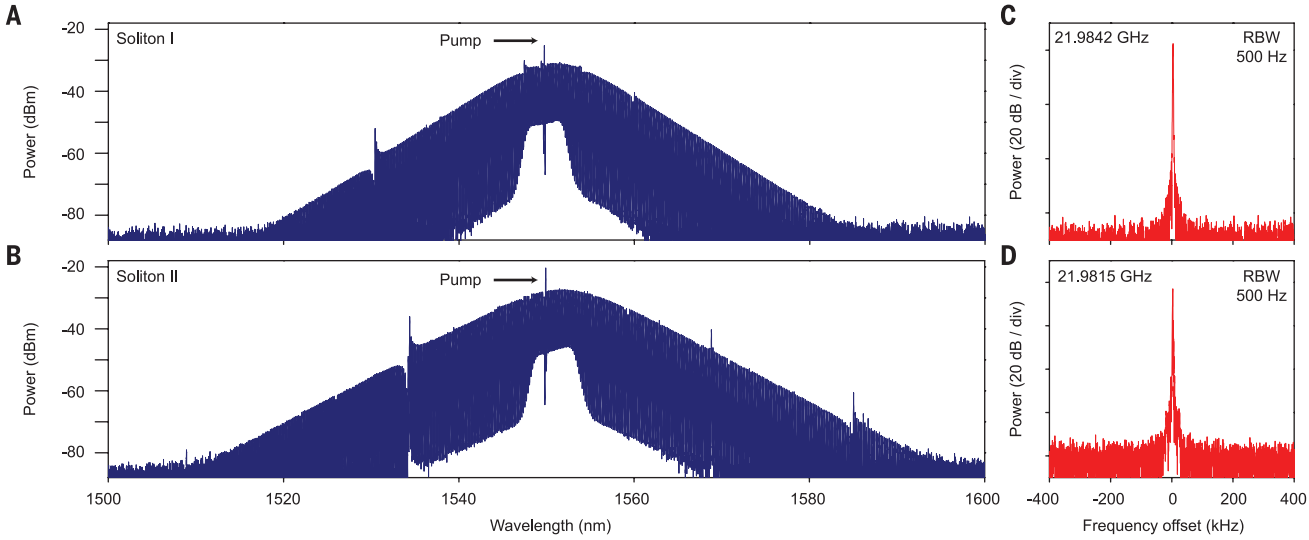

Fig. 2. Soliton comb spectral characterization. (**A** and **B**) Optical spectra of the microresonator soliton pulse streams. (**C** and **D**) Electrical spectra showing the repetition rates of the soliton pulse streams. The rates and resolution bandwidth (RBW) are given within the panels.

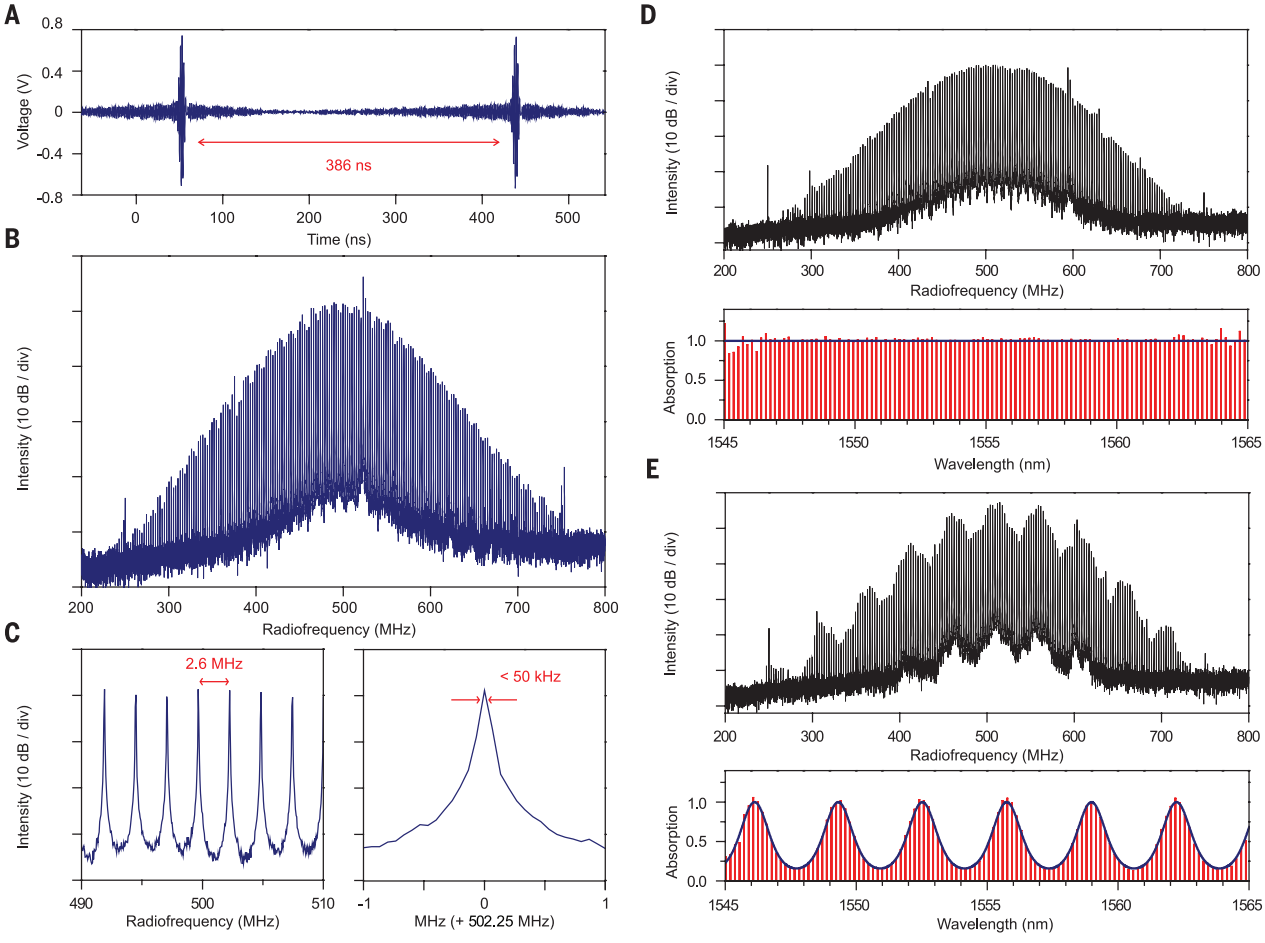

Fig. 3. Measured electrical interferogram and spectra. (**A**) The detected interferogram of the reference soliton pulse train. (**B**) Typical electrical spectrum obtained by Fourier transform of the temporal interferogram in (A). Ten spectra each are recorded over a time of 20 μs and averaged to obtain the displayed spectra. (**C**) Resolved (multiple and individual) comb lines of the spectrum in (B) are equidistantly separated by 2.6 MHz, the difference in the soliton repetition rate of the two microresonators. The linewidth of each comb line is <50 kHz and is set by the mutual coherence of the pumping lasers. (**D** and **E**) Fourier transform (black) of the signal interferogram produced by coupling the dual-soliton pulse trains through the synthetic absorber (WaveShaper; see fig. S1) with programmed absorption functions (spectrally flat and sine-wave). The obtained dual-comb absorption spectra (red) are compared with the programmed functions (blue curves) from 1545 to 1565 nm.

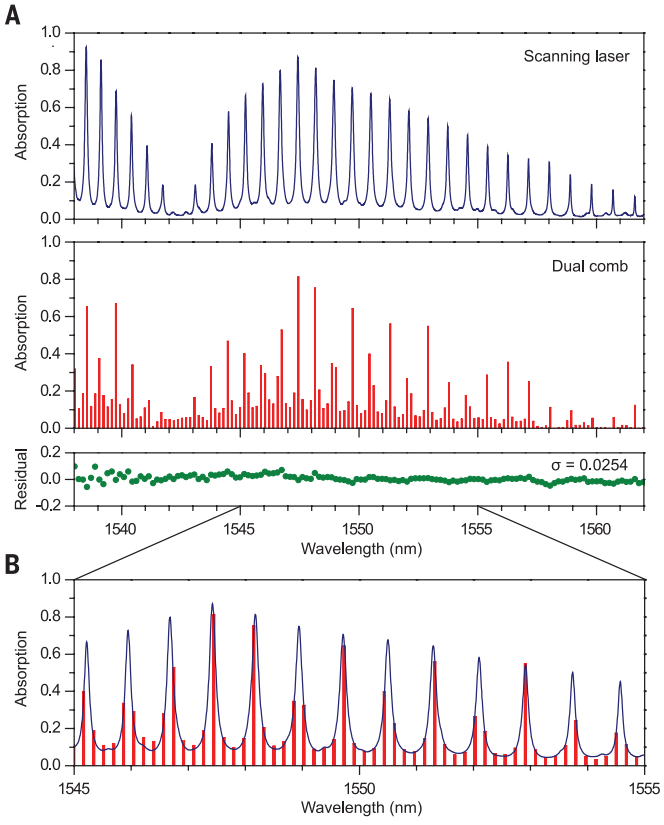

Fig. 4. Measured molecular absorption spectra. (**A**) Absorption spectrum of $2\nu_3$ band of $H^{13}CN$ measured by direct power transmission using a wavelength-calibrated scanning laser and comparison to the microresonator-based dual-comb spectrum. The residual difference between the two spectra is shown in green. (**B**) Overlay of the directly measured optical spectrum and the dual-comb spectrum, showing line-by-line matching. The vertical positions of the two spectra are adjusted to compensate for insertion loss.

measurement. The other path is coupled directly to a photodetector and functions as the reference. The test sample path also includes an alternate path (shown in fig. S1) in which a WaveShaper is inserted (*28*). Temperature control of one of the microresonators is used to tune the relative optical frequency difference of the two soliton streams. In our measurements, this difference was held below 1 GHz, allowing the observation of the temporal interferogram on an oscilloscope (bandwidth 1 GHz).

The reference interferogram (Fig. 3A) has a period of 386 ns, corresponding to a soliton repetition rate difference of 2.6 MHz. This relatively small repetition rate difference was made possible by precise control of the resonator diameter (and hence the resonator free spectral range) using calibrated wet etching of the silica (*29*). It was possible to fabricate disks with even more closely matched repetition rates (<100 kHz). Figure 3B shows the calculated Fourier transform of the interferogram. The small repetition rate difference on the much larger 22-GHz soliton repetition rate makes it possible to compress an optical span of 4 THz (1535 to 1567 nm) into 500 MHz of electrical spectrum. The measured wavelength span is actually narrower than the observable wavelength span of the original soliton pulse streams and is limited by the photodetector noise. The interferogram spectrum has a SNR around 30 dB near the central lines. A zoom-in of the spectrum (multi- and single-line) is shown in Fig. 3C. The electrical comb lines are equidistantly separated by 2.6 MHz and have a linewidth (full width at half maximum) of <50 kHz, limited by the mutual coherence of the independent fiber pump lasers. The pump laser line in a dissipative Kerr soliton is also a comb tooth in the soliton optical spectrum. As a result, the frequency jitter in each pump is transferred as an overall shift on the resulting soliton comb. Externally locking the two combs should reduce the observed linewidth in the interferogram spectrum.

The pump lines are placed toward the high-frequency side (near 550 MHz) of the spectral maximum in the interferogram spectrum (see Fig. 3B). In the optical spectra (Fig. 2, A and B), the pump is blue-detuned relative to the soliton spectral maximum [this occurs on account of the Raman self-frequency shift of the soliton (*24*)]. This spectral landmark shows that the relative spectral placement of the soliton combs is such that high optical frequencies are mapped to high interferogram frequencies. The way in which certain nonidealities in the soliton spectra map into the interferogram spectrum is also of interest. Specifically, there are avoided mode crossing–induced Fano-like spurs (*24*) in the soliton optical spectra (Fig. 2, A and B) occurring near 1535 nm, and this generates a corresponding feature at 750 MHz in Fig. 3B.

As an initial test of the dual-comb source, synthetic absorption spectra were programmed in a WaveShaper and then measured as dual-comb spectra (*28*). In Fig. 3, D and E, Fourier transforms of the signal interferograms produced using the synthetic absorber are shown. The two programmed functions are a spectrally flat 3-dB absorption and a sine-wave absorption having a 4-dB amplitude. The synthetic absorption spectra, obtained by normalizing the signal and reference electrical spectra, are compared with the programmed functions in Fig. 3, D and E. The ability to reconstruct these synthetic spectral profiles clearly demonstrates the reproducibility of the soliton spectral profile.

Finally, we studied the absorption spectrum of the $H^{13}CN$ $2\nu_3$ band. In Fig. 4A, the measured dual-comb absorption spectrum from 1538 to 1562 nm is shown in red and compared with a directly measured absorption spectrum shown in blue. Both absorption spectra are normalized. A laser locked to a molecular absorption line enabled absolute frequency calibration of the spectra (*28*). Sampling-induced choppiness of the dual-comb spectrum is caused by the relatively coarse spectral resolution of the solitons in comparison to the spectral scale of the $H^{13}CN$ absorption lines. Nonetheless, the characteristic envelope of the $H^{13}CN$ $2\nu_3$ band is clearly resolved. The residual difference between the two absorption spectra is shown in green in Fig. 4A; the calculated standard deviation is 0.0254. Furthermore, a line-by-line overlay of the measured optical and dual-comb spectra (Fig. 4B) confirms the wavelength precision and absorption intensity accuracy of the dual-comb source. The directly measured $H^{13}CN$ absorption spectrum is obtained by coupling an external cavity diode laser (ECDL) into the $H^{13}CN$ gas cell and then scanning the laser while monitoring the transmitted optical power. A separate signal is also tapped from the ECDL to function as a reference (*28*).

In principle, a soliton source with finer comb spacing (i.e., lower repetition frequency) is possible. Nonsoliton microcombs with mode spacings as narrow as 2.4 GHz have been demonstrated using the silica resonator platform (*16*). The use of electro-optical modulators to modulate the microcombs by a fraction of the repetition frequency is another possible way to create a finer spectral comb grid. Also, tuning of the combs is, in principle, possible so as to create a nearly continuous high-resolution absorption measurement.

The dual-comb source is centered near 1550 nm (in the C-band) for this work; however, operation at other wavelengths within the transmission window of silica is also possible. Moreover, using fiber nonlinear broadening or internal (resonator) dispersive wave generation (*25*), it should be possible to greatly extend the comb spectral span. Resonator dispersion engineering (*30*) can also be used to extend comb bandwidth. More generally, a wide range of materials are available for microcombs enabling access to mid-infrared spectra. With further improvements, it should also be possible to realize chip-based dual-comb coherent anti-Stokes Raman spectroscopy (CARS). The potential for monolithic integration with other devices makes soliton-based microcombs well suited for possible realization of a dual-comb spectroscopic system-on-a-chip.

REFERENCES AND NOTES

1. D. J. Jones *et al.*, *Science* **288**, 635–640 (2000).
2. R. Holzwarth *et al.*, *Phys. Rev. Lett.* **85**, 2264–2267 (2000).
3. S. A. Diddams *et al.*, *Science* **293**, 825–828 (2001).
4. S. Schiller, *Opt. Lett.* **27**, 766–768 (2002).
5. F. Keilmann, C. Gohle, R. Holzwarth, *Opt. Lett.* **29**, 1542–1544 (2004).

6. I. Coddington, W. C. Swann, N. R. Newbury, *Phys. Rev. Lett.* **100**, 013902 (2008).
7. P. Giaccari, J.-D. Deschênes, P. Saucier, J. Genest, P. Tremblay, *Opt. Express* **16**, 4347–4365 (2008).
8. B. Bernhardt *et al.*, *Nat. Photonics* **4**, 55–57 (2010).
9. T. Ideguchi, A. Poisson, G. Guelachvili, N. Picqué, T. W. Hänsch, *Nat. Commun.* **5**, 3375 (2014).
10. I. Coddington, N. Newbury, W. Swann, *Optica* **3**, 414 (2016).
11. P. Del'Haye *et al.*, *Nature* **450**, 1214–1217 (2007).
12. T. J. Kippenberg, R. Holzwarth, S. A. Diddams, *Science* **332**, 555–559 (2011).
13. I. S. Grudinin, N. Yu, L. Maleki, *Opt. Lett.* **34**, 878–880 (2009).
14. S. B. Papp, S. A. Diddams, *Phys. Rev. A* **84**, 053833 (2011).
15. Y. Okawachi *et al.*, *Opt. Lett.* **36**, 3398–3400 (2011).
16. J. Li, H. Lee, T. Chen, K. J. Vahala, *Phys. Rev. Lett.* **109**, 233901 (2012).
17. B. Hausmann, I. Bulu, V. Venkataraman, P. Deotare, M. Lončar, *Nat. Photonics* **8**, 369–374 (2014).
18. T. J. Kippenberg, S. M. Spillane, K. J. Vahala, *Phys. Rev. Lett.* **93**, 083904 (2004).
19. A. A. Savchenkov *et al.*, *Phys. Rev. Lett.* **93**, 243905 (2004).
20. A. Hugi, G. Villares, S. Blaser, H. C. Liu, J. Faist, *Nature* **492**, 229–233 (2012).
21. G. Villares, A. Hugi, S. Blaser, J. Faist, *Nat. Commun.* **5**, 5192 (2014).
22. M. Yu, Y. Okawachi, A. Griffith, M. Lipson, A. L. Gaeta, in *CLEO: Science and Innovations 2016* (Optical Society of America, 2016), paper JTh4B.5.
23. T. Herr *et al.*, *Nat. Photonics* **8**, 145–152 (2014).
24. X. Yi, Q.-F. Yang, K. Y. Yang, M.-G. Suh, K. Vahala, *Optica* **2**, 1078 (2015).
25. V. Brasch *et al.*, *Science* **351**, 357–360 (2016).
26. P.-H. Wang *et al.*, *Opt. Express* **24**, 10890–10897 (2016).
27. C. Joshi *et al.*, *Opt. Lett.* **41**, 2565–2568 (2016).
28. See supplementary materials on *Science* Online.
29. H. Lee *et al.*, *Nat. Photonics* **6**, 369–373 (2012).
30. K. Y. Yang *et al.*, *Nat. Photonics* **10**, 316–320 (2016).

ACKNOWLEDGMENTS

We thank N. Newbury and G. Scalari for helpful comments on this manuscript. Supported by the Defense Advanced Research Projects Agency under the PULSE and SCOUT programs, NASA, and the Kavli Nanoscience Institute.

SUPPLEMENTARY MATERIALS

www.sciencemag.org/content/354/6312/600/suppl/DC1
Materials and Methods
Supplementary Text
Fig. S1
References (*31*–*34*)

27 July 2016; accepted 29 September 2016
Published online 13 October 2016
10.1126/science.aah6516

OPTICAL PROCESSING

A coherent Ising machine for 2000-node optimization problems

Takahiro Inagaki,[1]* Yoshitaka Haribara,[2,3,4] Koji Igarashi,[5] Tomohiro Sonobe,[4,6] Shuhei Tamate,[4] Toshimori Honjo,[1] Alireza Marandi,[7] Peter L. McMahon,[7] Takeshi Umeki,[8] Koji Enbutsu,[8] Osamu Tadanaga,[8] Hirokazu Takenouchi,[8] Kazuyuki Aihara,[2,3] Ken-ichi Kawarabayashi,[4,6] Kyo Inoue,[5] Shoko Utsunomiya,[4] Hiroki Takesue[1]*

The analysis and optimization of complex systems can be reduced to mathematical problems collectively known as combinatorial optimization. Many such problems can be mapped onto ground-state search problems of the Ising model, and various artificial spin systems are now emerging as promising approaches. However, physical Ising machines have suffered from limited numbers of spin-spin couplings because of implementations based on localized spins, resulting in severe scalability problems. We report a 2000-spin network with all-to-all spin-spin couplings. Using a measurement and feedback scheme, we coupled time-multiplexed degenerate optical parametric oscillators to implement maximum cut problems on arbitrary graph topologies with up to 2000 nodes. Our coherent Ising machine outperformed simulated annealing in terms of accuracy and computation time for a 2000-node complete graph.

Combinatorial optimization is an important task for various applications such as drug discovery, resource optimization in wireless networks, and machine learning (*1*). Many such problems are known to be nondeterministic polynomial time (NP)–hard or NP-complete problems, which are considered difficult to solve efficiently with modern digital computers. Several heuristic or "greedy" algorithms have been proposed in the field of computer science to find the optimal or near-optimal solutions to those problems. Among such algorithms, simulated annealing (SA) has performed well in solving various types of combinatorial optimization problems (*2*). It is known that combinatorial optimization problems can be mapped onto ground-state search problems of the Ising model with polynomial resources (*3*). Several approaches have been proposed and demonstrated to find solutions to Ising problems using networks of artificial spins based on various physical systems (*4*–*7*).

A coherent Ising machine (CIM) is one such artificial Ising machine, in which a laser (*8*) or a degenerate optical parametric oscillator (DOPO) (*9*) represents an artificial spin. This proposal was motivated by early studies on the quantum behaviors of a DOPO (*10*–*14*), and proof-of-principle CIM experiments have already been reported using time-multiplexed DOPOs (*15*, *16*). To date, physical Ising machines (*4*–*7*) have suffered from a limited number of spin-spin couplings due to localized spin implementations. For example, in a recent quantum annealing system based on 1152 superconducting qubits, the number of spin-spin couplings was 3360, constrained by the chimera graph structure (*17*). This limited number of spin-spin couplings has made it difficult to map various real-world optimization problems to the hardware. Here, we report a CIM that consists of 2048 DOPOs with full spin-spin couplings. A measurement and feedback (MFB) scheme enabled us to implement all possible connections among 2048 spins, which amounts to 2,096,128 spin-spin couplings, making it possible to solve arbitrary graph problems.

An Ising Hamiltonian without an external magnetic field is given by

$$H(\sigma) = -\sum_{i<j} J_{ij}\sigma_i\sigma_j \quad (1 \le i, j \le N) \qquad (1)$$

(*18*), where $\sigma_i \in \{-1,+1\}$ denotes the ith Ising spin, J_{ij} is the interaction strength between the ith and jth spins, and N is the total number of spins. The Ising machines described above are designed to find the ground state or low-energy states of the Ising Hamiltonian. A DOPO takes only a 0 or π phase relative to the pump phase above the threshold, so it can be used as a stable artificial spin realized with photonics technologies (*19*–*22*). A CIM solves the Ising problem according to the minimum-gain principle (*8*). According to this principle, if the optical couplings between the DOPOs are adjusted to implement $\{J_{ij}\}$, the DOPO network oscillates in the phase configuration with the lowest loss, which corresponds to the ground state of the Ising Hamiltonian in Eq. 1.

The size of the problem that a CIM can handle is determined by the number of DOPOs and their couplings. Delayed interferometers were used to couple the DOPOs in the previous CIM experiments (*15*, *16*); however, this scheme does not scale as the problems become more complex. To avoid this issue, Haribara *et al.* proposed an MFB scheme that makes it possible to couple any combination of N DOPOs (*23*).

Figure 1 shows a schematic of a CIM with MFB (*24*). The CIM uses a periodically poled lithium niobate (PPLN) waveguide, which is placed in a

[1]NTT Basic Research Laboratories, NTT Corporation, 3-1 Morinosato Wakamiya, Atsugi, Kanagawa 243-0198, Japan. [2]Department of Mathematical Informatics, University of Tokyo, Hongo 7-3-1, Bunkyo-ku, Tokyo 113-8656, Japan. [3]Institute of Industrial Science, University of Tokyo, 4-6-1, Komaba, Meguro-ku, Tokyo 153-8505, Japan. [4]National Institute of Informatics, Hitotsubashi 2-1-2, Chiyoda-ku, Tokyo 101-8403, Japan. [5]Division of Electrical, Electronic and Information Engineering, Osaka University, Osaka 565-0871, Japan. [6]ERATO Kawarabayashi Large Graph Project, Japan Science and Technology Agency, Hitotsubashi 2-1-2, Chiyoda-ku, Tokyo 101-8403, Japan. [7]E. L. Ginzton Laboratory, Stanford University, Stanford, CA 94305, USA. [8]NTT Device Technology Laboratories, NTT Corporation, 3-1 Morinosato Wakamiya, Atsugi, Kanagawa 243-0198, Japan.
***Corresponding author. Email: inagaki.takahiro@lab.ntt.co.jp (T.I.); takesue.hiroki@lab.ntt.co.jp (H.T.)**

Microresonator soliton dual-comb spectroscopy

Myoung-Gyun Suh, Qi-Fan Yang, Ki Youl Yang, Xu Yi and Kerry J. Vahala

Science **354** (6312), 600-603.
DOI: 10.1126/science.aah6516originally published online October 13, 2016

Shrinking spectrometers

Dual-comb spectroscopy is a powerful technique that uses the interference of two closely related combs to map spectroscopic features directly into a frequency domain that can be read by electronics. Suh *et al.* developed a dual-comb spectroscopy approach using combs produced by silica microresonators fabricated on a silicon chip. Perhaps high-resolution spectroscopy will soon be shrunk to the chip scale, doing away with the need for bulky spectrometers.

Science, this issue p. 600